



In situ, high-resolution evidence of phosphorus release from sediments controlled by the reductive dissolution of iron-bound phosphorus in a deep reservoir, southwestern China

Quan Chen^{a,b}, Jingan Chen^{a,*}, Jingfu Wang^a, Jianyang Guo^a, Zuxue Jin^{a,c}, Pingping Yu^{a,c}, Zhenzhen Ma^{a,d}

^a State Key Laboratory of Environmental Geochemistry, Institute of Geochemistry, Chinese Academy of Sciences, Guiyang 550081, PR China

^b University of Chinese Academy of Sciences, Beijing 100049, PR China

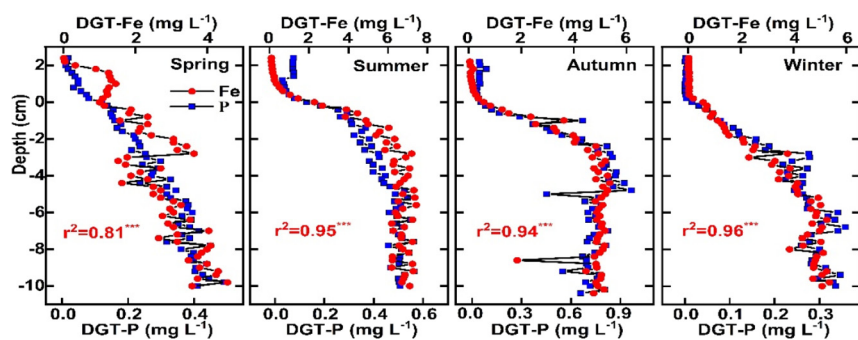
^c College of Resource and Environmental Engineering, Guizhou University, Guiyang 550025, PR China

^d Xi'an University of Science and Technology, Xi'an 710054, PR China

HIGHLIGHTS

- In situ, millimeter scale investigation on monthly variation of the labile P (Fe) at the SWI was first carried out using DGT in a deepwater reservoir, southwestern China.
- Significant positive correlation between DGT-labile P and DGT-labile Fe in sediments indicated that P release is controlled by the reductive dissolution of iron-bound P.
- The apparent P diffusion flux at the SWI was remarkably high, with a mean value of $0.22 \text{ mg} \cdot \text{m}^{-2} \cdot \text{d}^{-1}$, highlighting the importance of the internal P pollution.

GRAPHICAL ABSTRACT



ARTICLE INFO

Article history:

Received 29 November 2018

Received in revised form 3 February 2019

Accepted 12 February 2019

Available online 13 February 2019

Editor: Filip M.G. Tack

Keywords:

Eutrophication

Phosphorus

Sediments

Diffusive gradients in thin films (DGT)

Deep reservoirs

Southwestern China

ABSTRACT

Reservoirs in southwestern China are encountering the challenge of eutrophication, in which internal phosphorus (P) release from sediments plays an important role. Studies on the high-resolution profile variations and release mechanisms of P at the sediment-water interface (SWI) are rare in these reservoirs until now. In this study, monthly monitoring (Nov 2017 to Oct 2018) using a composite diffusive gradient in thin films (DGT) technique was taken to determine the temporal and vertical profile variations of the DGT-labile P (Fe) at the SWI in Hongfeng Reservoir. The results showed that the average concentrations of the DGT-labile P (Fe) in surface sediments were $0.63 \pm 0.24 \text{ mg} \cdot \text{L}^{-1}$ and $4.61 \pm 1.12 \text{ mg} \cdot \text{L}^{-1}$, respectively, with significantly higher concentrations during the summer anoxic period than that during the winter aerobic period. The DGT-labile P (Fe) concentrations in sediments presented a significant positive correlation ($r^2 > 0.70$, $p < 0.001$), supporting the simultaneous release of reactive P and reactive Fe from the sediments and indicating that the reductive dissolution of iron-bound P dominates the P release from sediments. The release rates of P ranged from $0.01 \text{ mg} \cdot \text{m}^{-2} \cdot \text{d}^{-1}$ to $0.83 \text{ mg} \cdot \text{m}^{-2} \cdot \text{d}^{-1}$ (mean: $0.22 \text{ mg} \cdot \text{m}^{-2} \cdot \text{d}^{-1}$) in Hongfeng Reservoir, which are higher than that in heavily eutrophic shallow lakes in eastern China, such as Lake Taihu. There is a higher P loading, stronger P reactivity, faster P release rates, and higher pollution potential in deep reservoirs of southwestern China than that in natural shallow lakes of eastern China, highlighting the importance and urgency of treating internal P pollution in deep reservoirs. Further studies on the mechanisms and controlling factors of the coupled Fe-P-S cycle in deep reservoirs

* Corresponding author.

E-mail address: chenjingan@vip.skleg.cn (J. Chen).

are desirable in the future, so as to provide a scientific foundation for exploring effective internal P treatment techniques adaptive to deep reservoirs in southwestern China.

© 2019 Elsevier B.V. All rights reserved.

1. Introduction

As an important form of water resource utilization, reservoirs of different sizes have been constructed on 70% of the rivers globally (Kummu and Varis, 2007). By the end of 2011, China has constructed 97,624 reservoirs with a total water storage capacity over $8.1 \times 10^{11} \text{ m}^3$, ranking first in the world for the number of reservoirs (Lehner et al., 2011; Wang et al., 2018a). Southwestern China is enriched in hydro-power resources with numerous reservoirs. However, these reservoirs are encountering the challenge of eutrophication (Ni and Wang, 2015; Chen et al., 2018a, 2018b). Previous studies have demonstrated that phosphorus (P) is a key limiting factor in the eutrophication of water body (Lewis et al., 2011; Schindler et al., 2016; Chen et al., 2018a, 2018b; Ding et al., 2018). After external P loading has been effectively controlled, the release of P from sediments (internal P loading) could still cause the water body to maintain a eutrophic state for decades (Paytan et al., 2017).

The impoundment of reservoir usually floods large grassland, woodland, and farmland areas, which forms a new unstable sediment-water interface (SWI) and accelerates the release of nutrients, such as nitrogen (N) and P. Most reservoirs in southwestern China are deepwater reservoirs with a mean depth of 10–50 m (Chen et al., 2018a, 2018b). The release of P from sediments in these deep reservoirs can be divided into two stages. First, the reactive P in the solid-phase sediments is desorbed and released into the pore water (Monbet et al., 2008; Ding et al., 2015). Second, phosphate in the pore water freely diffuses toward the overlying water, driven by the concentration gradient at the SWI (Wu et al., 2001; Xu et al., 2012).

The biogeochemical behavior of P at the SWI in lakes has been studied extensively. As early as the 1940s, Mortimer (1942) hypothesized that a coupled cycle occurs between iron (Fe) and P. Since the publication of Mortimer's (1942) study, the simultaneous release of Fe and P from sediments has been reported in many natural lakes (Christophoridis and Fytianos, 2006; Smith et al., 2011; Ding et al., 2016), revealing that the reductive dissolution of iron-bound P plays a crucial role in the migration and transformation of the internal P. Besides, the dissolution of calcium-bound P (Mayer et al., 1999; Chen et al., 2015a, 2015b), the mineralization of P-containing organic matter (Golterman, 2001) and the degradation of polyphosphates (Hupfer et al., 2007) in sediments were demonstrated to be important mechanisms of the activation and release of P. The biogeochemical behavior of P is affected by various physical, chemical, and biological factors, such as temperature, dissolved oxygen (DO), pH, bacterial activity, contents of Fe, aluminum (Al), and calcium (Ca), enzymatic hydrolysis reactions and hydrodynamics (Amirbahman et al., 2003; Smolders et al., 2006; Schroth et al., 2015; Chen et al., 2015a, 2015b, 2016).

Previous studies on processes and mechanisms behind the release of P were mostly focused on natural lakes (Ding et al., 2016; Gao et al., 2016), while high-resolution investigations on the temporal and vertical profile variations and the release mechanisms of P at the SWI in deep reservoirs are rare. In previous studies, after the collection of sediments cores, the physical-chemical properties of the sediments inevitably changed during transportation, storage and chemical analysis in the laboratory (Rydin, 2000). In this study, a composite DGT technique (Zhang and Davison, 1995; Xu et al., 2013; Ding et al., 2016) was used for monthly *in-situ* monitoring (Nov 2017 to Oct 2018) to determine the concentration profiles of the DGT-labile P (Fe) at the SWI in Hongfeng Reservoir, a deep eutrophic reservoir in southwestern China. After the sediments core was collected, the DGT probe was inserted and then the core was immediately returned to the bottom of

the lake for *in-situ* culture by means of a tripod lander. Recovery and chemical analysis was performed after 24 h, which improves the measurement accuracy. The objectives of this study are: 1) to clarify the temporal and vertical profile variations in the concentrations of DGT-labile P (Fe) at the SWI in Hongfeng Reservoir; 2) to reveal the migration mechanism and release flux of P; and 3) to get a deep insight into the P pollution in deep reservoirs, southwestern China.

2. Materials and methods

2.1. Study site and sample collection

Hongfeng Reservoir (26°26'–26°35' N, 106°19'–106°28' E) is located in the southwestern plateau of China. In Hongfeng Reservoir, the average water depth is approximately 11 m, the water area is 57.2 km² and the total storage capacity is $6.01 \times 10^8 \text{ m}^3$. It is the main source of drinking water for Guiyang, the capital city of Guizhou Province (Fig. 1). Hongfeng Reservoir was constructed for water storage in the 1960s. Over the past decades, the discharge of industrial wastewater, agricultural non-point source pollution and urban domestic sewage resulted in water quality deterioration. At present, Hongfeng Reservoir is in a state of mesotrophication. The ratio of total N (TN) to total P (TP) is approximately 40:1, presenting a typical P-restricted eutrophic water body (Wang et al., 2016). The TP content in surface sediments in Hongfeng Reservoir varied from 770 mg·kg⁻¹ to 4310 mg·kg⁻¹, with an average content as high as 1820 mg·kg⁻¹ (Wang et al., 2016).

From Nov 2017 to Oct 2018, sediments cores were collected in the southern center (SC; water depth: 16 m) and northern center (NC; water depth: 23 m) monthly (Fig. 1) using a gravity sampler. After the cores were collected, the bottom was sealed with a rubber stopper. The ZrO-Chelex DGT probe was inserted vertically into the surface sediments. Within 15 min, the cores were fixed in the center of the self-developed tripod lander and then the lander was slowly placed at the surface mud of the original sampling point with nylon ropes. The buoys were connected to ropes, which served as marks for easy retrieval. At the same time, samples of stratified water were taken at intervals of 2–4 m. The water samples were sealed and brought back to the laboratory for chemical analysis.

2.2. Preparation and deployment of ZrO-Chelex DGT probes

The ZrO-Chelex DGT was composed of a fixing plate, gel combining layer, agar diffusive layer, micro-porous filtrating film (pore size: 0.45 μm, thickness: 0.10 mm) (EasySensor Ltd., Nanjing, China). The device can simultaneously obtain sub-micron concentration profiles of reactive P and reactive Fe(II) at SWI, with maximum capacities of 75 μg·cm⁻² and 90 μg·cm⁻², respectively (Xu et al., 2013). After 24 h, the core with the inserted ZrO-Chelex DGT was retrieved, sealed, refrigerated and then brought back to the laboratory for chemical analysis.

2.3. Chemical analysis

The retrieved ZrO-Chelex DGT samples were analyzed according to the methods reported by Xu et al. (2013). The surface of the ZrO-Chelex gels were washed with deionized water and the samples were cut with a ceramic knife at intervals of 2 mm (EasySensor Ltd., Nanjing, China). The slices of the thin film were transferred to a 1.5 mL centrifuge tube. Next, 0.8 mL of 1 mol·L⁻¹ nitric acid and 1 mol·L⁻¹ sodium hydroxide solution was used to extract reactive Fe(II) and reactive P components over 16 h, respectively.

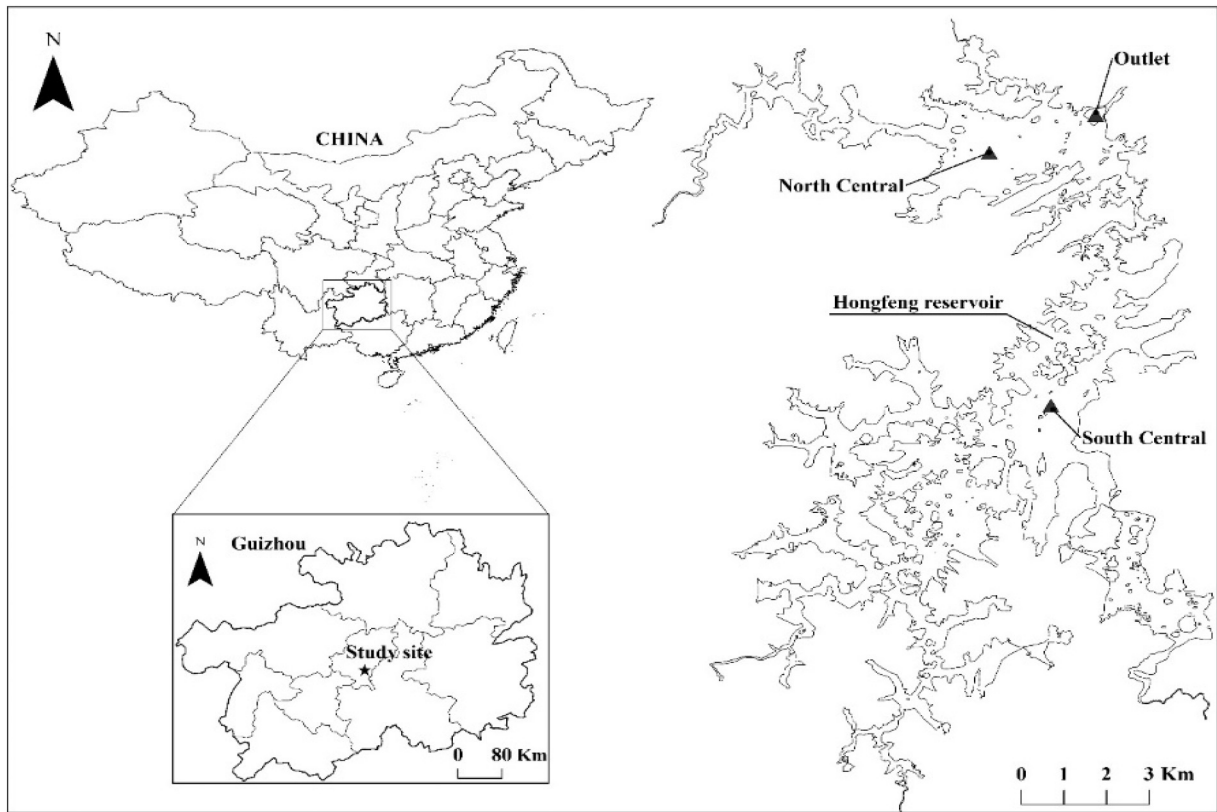


Fig. 1. Location of Hongfeng Reservoir and sampling sites.

The concentrations of DGT-labile P (Fe) were determined by miniaturized spectrophotometry method (Epoch Microplate Spectrophotometer, Biotek, USA) as described by Xu et al. (2012). The concentrations of TP and soluble reactive P (SRP) in the overlying water were determined by the molybdenum blue method (Murphy and Riley, 1962). Concentrations of Fe(II) in the DGT elutes were determined using the phenanthroline colorimetric method (Tamura et al., 1974). The temperature, DO and pH of the stratified water was measured *in-situ* at 1 m intervals using a portable multi-parameter water quality meter (YSI 6600V2, YSI Ltd., USA).

2.4. Data analysis

According to Eq. (1), the concentrations of reactive P and reactive Fe (II) in the sediments obtained through DGT can be calculated as (Zhang and Davison, 1995):

$$C_{DGT} = \frac{M\Delta g}{DA t} \quad (1)$$

where, C_{DGT} represents the concentration of target matter ($\text{mg}\cdot\text{L}^{-1}$); M represents the accumulated amount of ZrO-Chelex DGT thin film ($\mu\text{g}\cdot\text{cm}^{-2}$) within the sampling time; Δg is the thickness (cm) of the film's diffusion layer; D is the diffusion coefficient ($\text{cm}^2\cdot\text{s}^{-1}$) at the corresponding temperature; A represents the sampling area (cm^2); and t is the sampling time (s).

According to the concentration profile of DGT-labile P at the SWI, the apparent diffusion flux (F_d) of P in the sediments can be calculated (Ding et al., 2015; Eq. (2)):

$$F_d = J_w + J_s = -D_w \left(\frac{\partial C_{DGT}}{\partial X_w} \right)_{(x=0)} - \varphi D_s \left(\frac{\partial C_{DGT}}{\partial X_s} \right)_{(x=0)} \quad (2)$$

where, J_w and J_s is the diffusive fluxes through the SWI of the overlying water and sediments, respectively; D_w and D_s is the diffusion coefficients

of phosphates in the overlying water and sediments, respectively; and $\left(\frac{\partial C_{DGT}}{\partial X_w} \right)_{(x=0)}$ and $D_s \left(\frac{\partial C_{DGT}}{\partial X_s} \right)_{(x=0)}$ is the concentration gradients of DGT-labile P in overlying water and sediments, respectively.

To obtain the precise flux value, the concentration gradients were calculated from the DGT-labile P concentration profiles at the SWI (± 5 mm). According to Eq. (3), the diffusion coefficient (D_s) of phosphates in the sediments can be calculated as (Ullman and Aller, 1982):

$$D_s = \frac{D_w}{\varphi F} \quad (3)$$

where, φ is the porosity of the sediments; F is the strata's coefficient of resistivity; D_w is the diffusion coefficient of phosphate in water, which can be calculated according to the on-time temperature (Yuan-Hui and Gregory, 1974). The strata's coefficient of resistivity F is determined by the porosity of sediment (φ). When $\varphi \geq 0.7$, $F = 1/\varphi^3$; $\varphi < 0.7$, $F = 1/\varphi^2$ (Ullman and Aller, 1982; Yuan-Hui and Gregory, 1974).

2.5. Statistical analyses

SPSS was used to perform statistical analysis. The Pearson correlation coefficient was determined to analyze the correlation between DGT-labile P and DGT-labile Fe. Origin was used to plot the processed data.

3. Results

3.1. Physio-chemical property of hypolimnetic water

Water quality characteristics of the bottom water are summarized in Fig. 2. The lowest water temperature (SC: 7.5 °C; NC: 7.9 °C) of the bottom water was recorded in Mar 2018, and the highest was recorded in Aug 2018 (SC: 21.5 °C) and Sep 2018 (NC: 21.3 °C), respectively. From

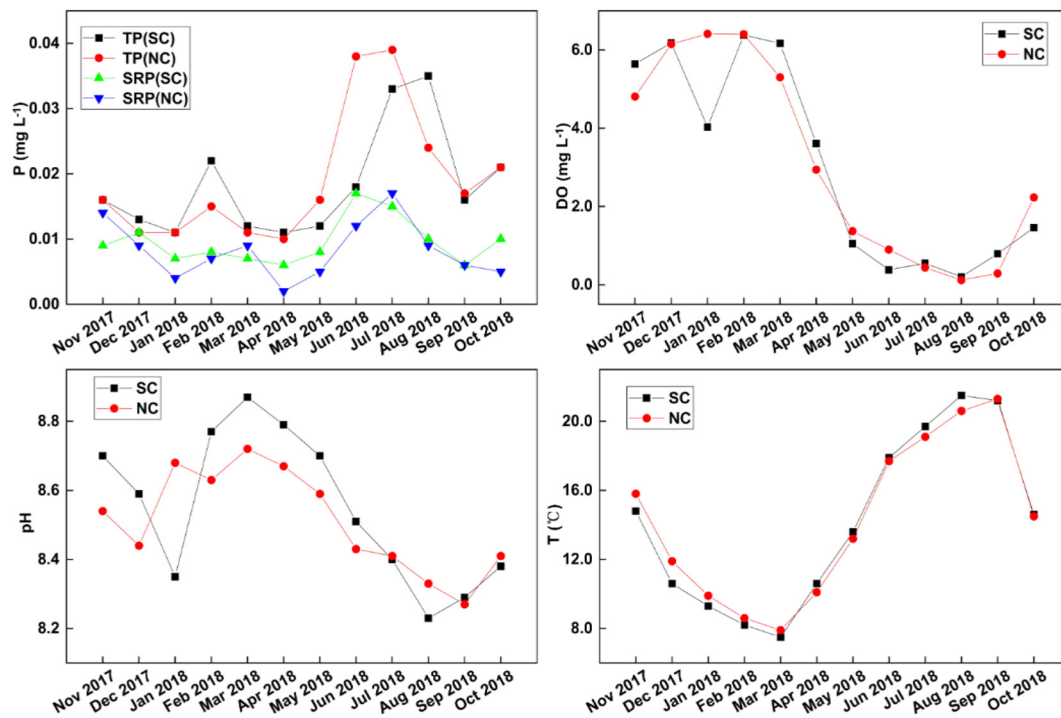


Fig. 2. Variations of total phosphorus (TP), soluble reactive phosphorus (SRP), dissolved oxygen (DO), pH, and temperature (T) in hypolimnetic water of Hongfeng Reservoir.

Nov 2017 to Apr 2018, the bottom of the reservoir was in an aerobic condition ($DO > 4 \text{ mg} \cdot \text{L}^{-1}$) with a maximum DO concentration of $6.41 \text{ mg} \cdot \text{L}^{-1}$. From May 2018 to Oct 2018, the bottom water was in a hypoxic condition ($DO < 2 \text{ mg} \cdot \text{L}^{-1}$) (Alvisi and Cozzi, 2016) with a lowest DO concentration of $0.12 \text{ mg} \cdot \text{L}^{-1}$. The bottom water was weakly alkaline, with pH ranging from 8.23 to 8.87. The TP concentrations in the bottom water in SC were 0.012, 0.029, 0.018 and $0.015 \text{ mg} \cdot \text{L}^{-1}$ in spring, summer, autumn, and winter respectively, and those in NC were 0.012, 0.034, 0.025 and $0.012 \text{ mg} \cdot \text{L}^{-1}$, respectively. The mean TP concentration in the bottom water during the hypoxic period increased by 142% (SC) and 183% (NC) compared to that during the aerobic period.

3.2. Temporal and vertical profile variations of DGT-labile P (Fe) concentrations

Temporal and vertical profile variations of the DGT-labile P (Fe) concentrations at the SWI are summarized in Fig. 3. Coincident variations of the DGT-labile P (Fe) concentrations in the vertical profile displayed the characteristics of first increasing and then stabilizing or decreasing. In summer and autumn, the peak concentrations of DGT-labile P (Fe) presented in the upper sediments layer, while occurred in the middle and lower layers in winter and spring. The highest (lowest) DGT-labile P and Fe concentrations were recorded in summer (winter) in both sites. The concentrations of DGT-labile P (Fe) in SC in summer increased by 267%, 216% respectively, compared to that in winter, and those in NC was 133%, 130%, respectively.

Significant positive correlations were observed between DGT-labile P and DGT-labile Fe, except for the data collected in Mar 2018 (Table 1). The correlation coefficient (r^2) between DGT-labile P and DGT-labile Fe in SC in spring, summer, autumn, and winter was 0.83, 0.98, 0.90 and 0.93, respectively, and those in NC was 0.79, 0.89, 0.82 and 0.78, respectively. The remarkably low correlation coefficient ($r^2 = 0.07, 0.14$, respectively) was recorded in Mar 2018 in both SC and NC, indicating there is no significant correlation between DGT-labile P and DGT-labile Fe.

3.3. Estimation of the apparent diffusion flux of P across the SWI

The apparent fluxes of reactive P at the SWI are shown in Fig. 4. Significant differences were observed across the sampling times. Apparent fluxes varied from 0.01 to $0.83 \text{ mg} \cdot \text{m}^{-2} \cdot \text{d}^{-1}$, with the lowest level appearing in Feb 2018 ($0.01 \text{ mg} \cdot \text{m}^{-2} \cdot \text{d}^{-1}$) and the highest in Aug 2018 ($0.83 \text{ mg} \cdot \text{m}^{-2} \cdot \text{d}^{-1}$). The average apparent fluxes of reactive P at the SWI in SC in spring, summer, autumn, and winter were 0.19, 0.38, 0.34 and $0.04 \text{ mg} \cdot \text{m}^{-2} \cdot \text{d}^{-1}$, respectively, and those in NC were 0.16, 0.27, 0.17 and $0.07 \text{ mg} \cdot \text{m}^{-2} \cdot \text{d}^{-1}$, respectively.

4. Discussion

4.1. Biogeochemical behavior of P in sediments

Seasonal differences were observed on the concentrations of DGT-labile P (Fe) at the SWI, with high concentrations during the hypoxic period and low concentrations during the aerobic period (Fig. 3). The DO in the bottom water may be responsible for the seasonal variations of the DGT-labile P (Fe) concentrations (Gao et al., 2016; Wang et al., 2016; Chen et al., 2018a, 2018b). Previous studies have revealed that the reductive dissolution of iron-bound P in surface sediments could significantly increase the concentrations of P (Fe) in the bottom water during the hypoxic period (Mortimer, 1942; Christophoridis and Fytianos, 2006). An obvious physio-chemical stratification existed, and the bottom water was hypoxic in Hongfeng Reservoir in summer and autumn (Fig. 2). Previous studies showed that TP and total Fe contents decreased by 6.5% and 14.8% in surface sediments during the hypoxic period, respectively, compared to that in aerobic conditions (Wang et al., 2018a). The TP concentrations in the bottom water (Fig. 2) and the DGT-labile P (Fe) concentration were also increased in surface sediments (Fig. 3) during the hypoxic period.

Synchronous variations were observed between DGT-labile P and DGT-labile Fe in the vertical profile (Fig. 3). Under the aerobic conditions, Fe exists mainly in the form of Fe (III) oxide-hydroxide in surface sediments (Lewandowski and Hupfer, 2005). The low DGT-labile P (Fe)

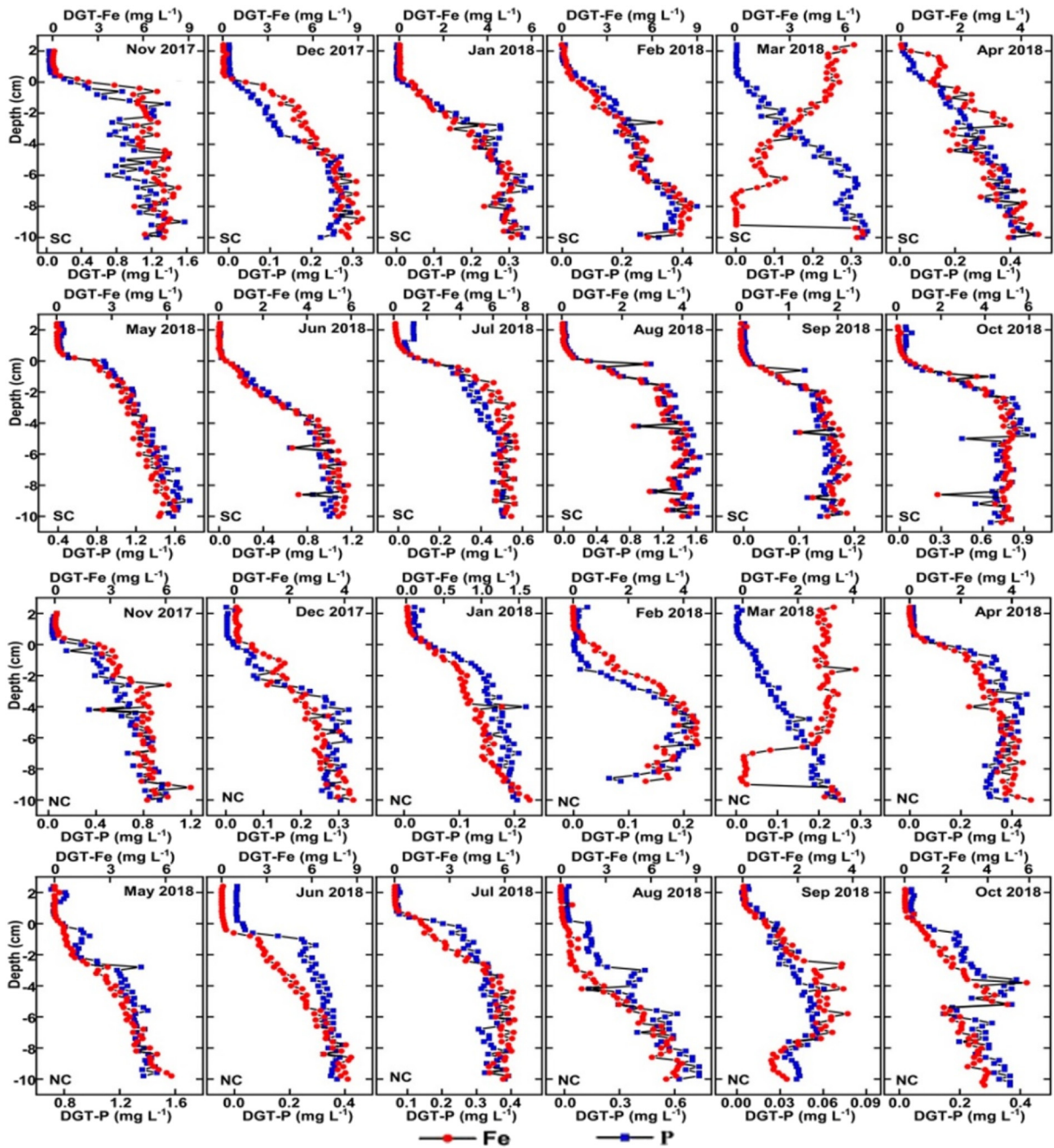


Fig. 3. Variations of the DGT-labile P (Fe) concentrations in sediments of Hongfeng Reservoir. The location of the sediment-water interface is represented by zero.

concentrations in surface sediments in winter could be attributed to the adsorption of phosphate by iron oxide-hydroxide and the formation of iron-bound P (Lewandowski et al., 2010). Due to the limited penetration depth of DO, the middle and lower sediments was still hypoxic in winter (Wang et al., 2016), therefore, the Fe(III) oxide-hydroxide in the sediments was reductively dissolved, resulting in high DGT-labile Fe

concentrations in the middle and lower sediments, and the DGT-labile P (Fe) concentrations exhibited an increasing trend toward the lower sediments in the vertical profile (Fig. 3). During the hypoxic period, the reductive dissolution of iron oxide-hydroxide occurred in surface sediments and led to the desorption of iron-bound P (Christophoridis and Fytianos, 2006), thus the DGT-labile P (Fe) concentrations were high in surface sediments in summer. Previous studies have revealed that microbial activities, especially the reductive activity of sulfate-reducing bacteria (SRB), are coupled with the geochemical cycle of P and Fe in sediments during the hypoxic period (Roden and Zachara, 1996). The sulfate reduction has a strong influence on the distribution of Fe in the vertical profile through the formation of the iron sulfides (FeS), thereby promoting the reduction of Fe(III) and inducing the desorption and release of iron-bound P in sediments indirectly (Sinkko et al., 2013; Wang et al., 2016). The bottom water in Hongfeng Reservoir

Table 1
Correlation between DGT-labile Fe and DGT-labile P ($p < 0.001$) in Hongfeng Reservoir.

	2017 Nov	2017 Dec	2018 Jan	2018 Feb	2018 Mar	2018 Apr	2018 May	2018 Jun	2018 Jul	2018 Aug	2018 Sep	2018 Oct
SC	0.78	0.91	0.96	0.92	0.07	0.81	0.99	0.98	0.95	1.00	0.98	0.94
NC	0.88	0.83	0.81	0.71	0.14	0.74	0.84	0.87	0.91	0.88	0.74	0.85

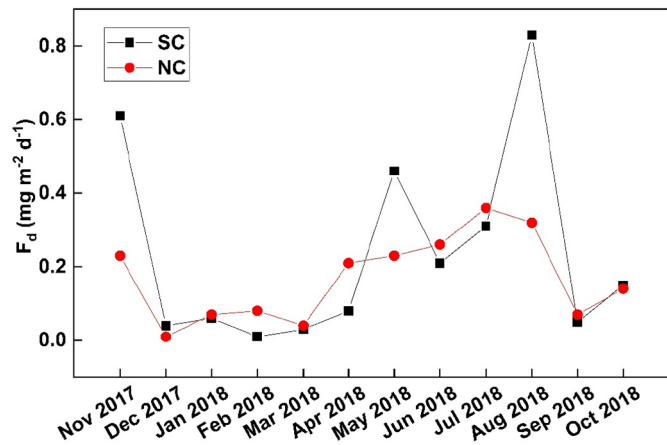


Fig. 4. The apparent diffusion fluxes of P at the sediment-water interface in SC and NC of Hongfeng Reservoir.

was hypoxic ($DO < 2 \text{ mg} \cdot \text{L}^{-1}$) from May 2018 to Oct 2018. Intense sulfate reduction may promote the desorption of iron-bound P in surface sediments, thus the peak DGT-labile P (Fe) concentrations occurred closer to the SWI in summer than that in winter (aerobic condition) (Fig. 3).

Significant positive correlations ($r^2 > 0.70$, $p < 0.001$; Table 1) were observed between DGT-labile P and DGT-labile Fe in the vertical profile, except for Mar 2018, which indicated that P and Fe were released simultaneously from sediments, supporting the viewpoint that P release is controlled by the reductive dissolution of iron-bound P (Zhang and Davison, 1995; Christophoridis and Fytianos, 2006; Xu et al., 2012). In March 2018, there was no significant correlation between DGT-labile P and DGT-labile Fe. Sediment re-suspension caused by hydrodynamic disturbances may be responsible for the abnormal phenomena (Schroth et al., 2015; Cheng and Hua, 2018; Wu et al., 2019). According to Hongfeng Power Station records, the reservoir opened to discharge water between Feb 25th and Mar 18th, 2018, which may cause a sharp increase of hydrodynamic force at the SWI and induce sediment re-suspension. A large amount of Fe(II) in disturbed surface sediments would be fixed by DGT probe. Therefore, the DGT-labile Fe concentrations in surface sediments were unusually high in March, significantly different from other months. Moreover, the Fe content in the sediments is approximately 30 times of the P content in Hongfeng Reservoir (Wang et al., 2018b). The released P during sediment re-suspension could be adsorbed effectively by iron oxide-hydroxide in surface sediments. Thus, the DGT-labile P concentrations in the surface sediment remain low in contrast to the DGT-labile Fe. Further study is needed to fully understand the unusual variations of the DGT-labile Fe (P) in March. In summary, the significant positive correlation of DGT-labile P (Fe) in the vertical profile indicated that the reductive dissolution of iron-bound P is the main mechanism of P release from sediments in Hongfeng Reservoir.

4.2. The influx of internal P loading

The apparent P diffusion flux at the SWI was remarkably high, with a mean value of $0.22 \text{ mg} \cdot \text{m}^{-2} \cdot \text{d}^{-1}$ (Fig. 4), which is significantly higher than that in shallow lakes, such as Lake Taihu (range: $-0.21 \text{ mg} \cdot \text{m}^{-2} \cdot \text{d}^{-1}$ to $0.65 \text{ mg} \cdot \text{m}^{-2} \cdot \text{d}^{-1}$; average: $0.15 \text{ mg} \cdot \text{m}^{-2} \cdot \text{d}^{-1}$) (Ding et al., 2015) and Lake Dongting (range: $-0.03 \text{ mg} \cdot \text{m}^{-2} \cdot \text{d}^{-1}$ to $0.20 \text{ mg} \cdot \text{m}^{-2} \cdot \text{d}^{-1}$; average: $0.09 \text{ mg} \cdot \text{m}^{-2} \cdot \text{d}^{-1}$) (Gao et al., 2016), indicating the seriousness of the internal P pollution in Hongfeng Reservoir. Although many shallow lakes in eastern China suffer from serious eutrophication, their internal P pollution level is relatively lower than that in deep reservoirs in southwestern China. For example, the TP contents in sediments of Lake Taihu

range from 360 to $950 \text{ mg} \cdot \text{kg}^{-1}$ (mean: $540 \text{ mg} \cdot \text{kg}^{-1}$). However, the TP contents are higher in deep reservoirs in southwestern China, such as Hongfeng Reservoir (range: 770 – $4310 \text{ mg} \cdot \text{kg}^{-1}$; mean: $1820 \text{ mg} \cdot \text{kg}^{-1}$), Baihua Reservoir (range: 1263 – $2815 \text{ mg} \cdot \text{kg}^{-1}$; mean: $1753 \text{ mg} \cdot \text{kg}^{-1}$) and Aha Reservoir (range: 1050 – $1960 \text{ mg} \cdot \text{kg}^{-1}$; mean: $1415 \text{ mg} \cdot \text{kg}^{-1}$) (Wu et al., 2001; Chen et al., 2018a, 2018b; Wang et al., 2018b). Furthermore, $>40\%$ of TP in sediments is labile components (i.e., iron-bound P) (Wang et al., 2018b) in deep reservoirs in southwestern China, increasing the environmental risks.

The internal P pollution is prominent in deep reservoirs of southwestern China for several reasons. Firstly, large amounts of grassland, woodland, and cultivated land were submerged during reservoir construction, forming a new unstable SWI where intensive material exchange happened and nutrients were released into the water body (Porvari, 1995; Chen et al., 2018a, 2018b). Secondly, most deep reservoirs (average water depth $> 10 \text{ m}$) are characterized by a seasonal physio-chemical stratification and hypoxic hypolimnion in summer and autumn, which accelerates the seasonal release of P from the sediments (Wang et al., 2016; Wang et al., 2018b). Finally, reservoirs are usually constructed in densely populated areas in order to provide social functions (irrigation, flood control, and tourism). The high ratio of basin to lake area of reservoirs increases the influx of artificial pollutants, including agricultural non-point source pollution, industrial wastewater, and domestic sewage. Thus, reservoirs usually have high pollutant input fluxes, resulting in high pollutant accumulation rates in sediments.

In short, there is a higher P loading, stronger P reactivity, faster P release rates, and higher pollution potential in deep reservoirs of southwestern China than that in natural shallow lakes of eastern China, highlighting the importance and urgency of treating internal P pollution in deep reservoirs. However, the internal P pollution in these deep reservoirs was usually neglected, because they were mostly built in recent 50 years and the environmental problems occurred only in recent ten years. After persistent accumulation of pollutants in sediments over the past decades, the internal P pollution becomes more and more serious and has an increasingly important influence on the water quality, deserving greater attention.

5. Conclusions

In-situ, millimeter scale investigation on the monthly variation of the labile P and Fe at the SWI was first carried out using DGT in a deep reservoir, southwestern China. Significant seasonal differences were observed in the DGT-labile P (Fe) concentrations at the SWI, which are higher during the hypoxic period and lower during the aerobic period. A significant positive correlation ($r^2 > 0.70$, $p < 0.001$) between DGT-labile P and DGT-labile Fe in sediments indicated that P release was controlled by the reductive dissolution of iron-bound P. The internal P release rate (mean: $0.22 \text{ mg} \cdot \text{m}^{-2} \cdot \text{d}^{-1}$) is higher in Hongfeng Reservoir than that in many shallow eutrophic lakes, such as Lake Taihu. There is a higher P loading, stronger P reactivity, faster P release rates, and higher pollution potential in deep reservoirs of southwestern China than that in natural shallow lakes of eastern China, highlighting the importance and urgency of treating internal P pollution in deep reservoirs. The environmental risks related to internal P release from sediments increase with the extension of a reservoir's running time, deserving greater attention.

The high-resolution dynamic sampling technique used in this study provides a deep insight on the micro-scale processes and mechanisms of P cycling in deep reservoirs, southwestern China. Further studies on the mechanisms and controlling factors of the coupled Fe-P-S cycle in deep reservoirs are desirable in the future, so as to provide a scientific foundation for exploring effective internal P treatment techniques adaptive to deep reservoirs in southwestern China.

Acknowledgements

This study was sponsored jointly by CAS Interdisciplinary Innovation Team of China, the Chinese NSF project (No. 41773145), the Youth Innovation Promotion Association CAS, and the Science and Technology Foundation of Guizhou Province, China ([2015]2001 and [2016]2802).

References

- Alvisi, F., Cozzi, S., 2016. Seasonal dynamics and long-term trend of hypoxia in the coastal zone of Emilia Romagna (NW Adriatic Sea, Italy). *Sci. Total Environ.* 541, 1448–1462.
- Amirbahman, A., Pearce, A.R., Bouchard, R.J., Norton, S.A., Kahl, J.S., 2003. Relationship between hypolimnetic phosphorus and iron release from eleven lakes in Maine, USA. *J. Anim. Plant Sci.* 65, 369–385.
- Chen, M., Ding, S., Liu, L., Xu, D., Han, C., Zhang, C.S., et al., 2015a. Iron-coupled inactivation of phosphorus in sediments by macrozoobenthos (chironomid larvae) bioturbation: evidences from high-resolution dynamic measurements. *Environ. Pollut.* 204, 241–247.
- Chen, F.X., Lu, S.Y., Jin, X.C., Guo, J.N., 2015b. Relationships of phosphorus forms in sediments of Fubao Gulf, Lake Dianchi, China. *J. Anim. Plant Sci.* 25, 190–196.
- Chen, M., Ding, S., Liu, L., Xu, D., Gong, M.D., Tang, H., et al., 2016. Kinetics of phosphorus release from sediments and its relationship with iron speciation influenced by the mussel (*Corbicula fluminea*) bioturbation. *Sci. Total Environ.* 542, 833–840.
- Chen, M., Ding, S., Chen, X., Sun, Q., Fan, X., Lin, J., et al., 2018a. Mechanisms driving phosphorus release during algal blooms based on hourly changes in iron and phosphorus concentrations in sediments. *Water Res.* 133, 153–164.
- Chen, J.A., Wang, J.F., Guo, J.Y., Yu, J., Zeng, Y., Yang, H.Q., et al., 2018b. Eco-environment of reservoirs in China: characteristics and research prospects. *Prog. Phys. Geogr.* 42, 185–201.
- Cheng, H.M., Hua, Z.L., 2018. Distribution, release and removal behaviors of tetrabromobisphenol A in water-sediment systems under prolonged hydrodynamic disturbances. *Sci. Total Environ.* 636, 402–410.
- Christophoridis, C., Fytianos, K., 2006. Conditions affecting the release of phosphorus from surface lake sediments. *J. Environ. Qual.* 35, 1181–1192.
- Ding, S., Han, C., Wang, Y., Yao, L., Wang, Y., Xu, D., Sun, Q., Williams, P.N., Zhang, C., 2015. In situ, high-resolution imaging of labile phosphorus in sediments of a large eutrophic lake. *Water Res.* 74, 100–109.
- Ding, S., Wang, Y., Wang, D., Li, Y.Y., Gong, M., Zhang, C., 2016. In situ, high-resolution evidence for iron-coupled mobilization of phosphorus in sediments. *Sci. Rep.* 6, 24341.
- Ding, S., Chen, M., Gong, M., Fan, X., Qin, B., Xu, H., et al., 2018. Internal phosphorus loading from sediments causes seasonal nitrogen limitation for harmful algal blooms. *Sci. Total Environ.* 625, 872–884.
- Gao, Y., Tao, L., Tian, S., Wang, L., Holm, P.E., Hansen, H.C.B., 2016. High-resolution imaging of labile phosphorus and its relationship with iron redox state in lake sediments. *Environ. Pollut.* 219, 466–474.
- Golterman, H.L., 2001. Phosphate release from anoxic sediments or 'what did Mortimer really write?'. *Hydrobiologia* 450, 99–106.
- Hupfer, M., Gloess, S., Grossart, H.P., 2007. Polyphosphate-accumulating microorganisms in aquatic sediments. *Aquat. Microb. Ecol.* 47, 299–311.
- Kummu, M., Varis, O., 2007. Sediment-related impacts due to upstream reservoir trapping, the lower Mekong River. *Geomorphology* 85, 275–293.
- Lehner, B., Liermann, C.R., Revenga, C., Vörösmarty, C., Fekete, B., Crouzet, P., et al., 2011. High-resolution mapping of the world's reservoirs and dams for sustainable river-flow management. *Front. Ecol. Environ.* 9, 494–502.
- Lewandowski, J., Hupfer, M., 2005. Effect of macrozoobenthos on two-dimensional small-scale heterogeneity of pore water phosphorus concentrations in lake sediments: a laboratory study. *Limnol. Oceanogr.* 50, 1106–1118.
- Lewandowski, J., Laskov, C., Hupfer, M., 2010. The relationship between Chironomus plumosus burrows and the spatial distribution of pore-water phosphate, iron and ammonium in lake sediments. *Freshw. Biol.* 52, 331–343.
- Lewis, W.M., Wurtsbaugh, W.A., Paerl, H.W., 2011. Rationale for control of anthropogenic nitrogen and phosphorus to reduce eutrophication of inland waters. *Environ. Sci. Technol.* 45, 10300–10305.
- Mayer, T., Ptacek, C., Zanini, L., 1999. Sediments as a source of nutrients to hypereutrophic marshes of Point Pelee, Ontario, Canada. *Water Res.* 33, 1460–1470.
- Monbet, P., Mckelvie, I.D., Worsfold, P.J., 2008. Combined gel probes for the in situ determination of dissolved reactive phosphorus in porewaters and characterization of sediment reactivity. *Environ. Sci. Technol.* 42, 5112–5117.
- Mortimer, C.H., 1942. The exchange of dissolved substances between mud and water in lakes. *J. Ecol.* 30, 147–201.
- Murphy, J., Riley, J.P., 1962. A modified single solution method for the determination of phosphate in natural waters. *Anal. Chim. Acta* 26, 31–36.
- Ni, Z.K., Wang, S.R., 2015. Historical accumulation and environmental risk of nitrogen and phosphorus in sediments of Erhai Lake, Southwest China. *Ecol. Eng.* 79, 42–53.
- Paytan, A., Roberts, K., Watson, S., Peek, S., Chuang, P.C., Defforey, D., et al., 2017. Internal loading of phosphate in Lake Erie Central Basin. *Sci. Total Environ.* 579, 1356–1365.
- Porvari, P., 1995. Mercury levels of fish in Tucuruí hydroelectric reservoir and in river Mojú in Amazonia, in the state of Pará, Brazil. *Sci. Total Environ.* 175, 109–117.
- Roden, E.E., Zachara, J.M., 1996. Microbial reduction of crystalline iron(III) oxides: influence of oxide surface area and potential for cell growth. *Environ. Sci. Technol.* 30, 1618–1628.
- Rydin, E., 2000. Potentially mobile phosphorus in Lake Erken sediment. *Water Res.* 34, 2037–2042.
- Schindler, D.W., Carpenter, S.R., Chapra, S.C., Hecky, R.E., Orihel, D.M., 2016. Reducing phosphorus to curb Lake eutrophication is a success. *Environ. Sci. Technol.* 50, 8923–8929.
- Schroth, A.W., Giles, C.D., Isles, P.D.F., et al., 2015. Dynamic coupling of iron, manganese and phosphorus behavior in water and sediment of shallow ice-covered eutrophic lakes. *Environ. Sci. Technol.* 49, 9758–9767.
- Sinkko, H., Luukkari, K., Sihvonen, L.M., Sivonen, K., Leivuori, M., Rantanen, M., et al., 2013. Bacteria contribute to sediment nutrient release and reflect progressed eutrophication-driven hypoxia in an organic-rich continental sea. *PLoS One* 8 (6), 61–67.
- Smith, L., Watzin, M.C., Druschel, G., 2011. Relating sediment phosphorus mobility to seasonal and diel redox fluctuations at the sediment-water interface in a eutrophic freshwater lake. *Limnol. Oceanogr.* 56, 2251–2264.
- Smolders, A.J.P., Lamers, L.P.M., Lucassen, E.C.H.E.T., Van Der Velde, G., Roelofs, J.G.M., 2006. Internal eutrophication: how it works and what to do about it — a review. *Chem. Ecol.* 22 (2), 93–111.
- Tamura, H., Goto, K., Yotsuyanagi, T., Nagayama, M., 1974. Spectrophotometric determination of iron(II) with 1,10-phenanthroline in the presence of large amounts of iron(III). *Talanta* 21, 314–318.
- Ullman, W.J., Aller, R.C., 1982. Diffusion coefficients in nearshore marine sediments. *Limnol. Oceanogr.* 27, 552–556.
- Wang, J.F., Chen, J.A., Ding, S.M., Guo, J.Y., Christopher, D., Dai, Z.H., et al., 2016. Effects of seasonal hypoxia on the release of phosphorus from sediments in deep-water ecosystem: a case study in Hongfeng reservoir, Southwest China. *Environ. Pollut.* 219, 858–865.
- Wang, F., Maberly, S.C., Wang, B., Liang, X., 2018a. Effects of dams on riverine biogeochemical cycling and ecology. *Inland Waters* 8, 130–140.
- Wang, J.F., Chen, J.A., Chen, Q., Yang, H.Q., Zeng, Y., Yu, P.P., et al., 2018b. Assessment on the effects of aluminum-modified clay in inactivating internal phosphorus in deep eutrophic reservoirs. *Chemosphere* 215, 657–667.
- Wu, F., Qing, H., Wan, G., 2001. Regeneration of N, P and Si near the sediment-water interface of lakes from southwestern China plateau. *Water Res.* 35, 1334–1337.
- Wu, T., Qin, B., Brookes, J.D., Yan, W., Ji, X., Feng, J., 2019. Spatial distribution of sediment nitrogen and phosphorus in Lake Taihu from a hydrodynamics-induced transport perspective. *Sci. Total Environ.* 650, 1554–1565.
- Xu, D., Wu, W., Ding, S., Sun, Q., Zhang, C., 2012. A high-resolution dialysis technique for rapid determination of dissolved reactive phosphate and ferrous iron in pore water of sediments. *Sci. Total Environ.* 421–422, 245–252.
- Xu, D., Chen, Y., Ding, S., Sun, Q., Wang, Y., Zhang, C., 2013. Diffusive gradients in thin films technique equipped with a mixed binding gel for simultaneous measurements of dissolved reactive phosphorus and dissolved iron. *Environ. Sci. Technol.* 47, 10477–10484.
- Yuan-Hui, L., Gregory, S., 1974. Diffusion of ions in sea water and in deep-sea sediments. *Geochim. Cosmochim. Acta* 38, 703–714.
- Zhang, H., Davison, W., 1995. Performance characteristics of diffusion gradients in thin films for the in situ measurement of trace metals in aqueous solution. *Anal. Chem.* 67, 3391–3400.